Characterisation, Analysis and Design Optimisation of a Wide Field-of-View Laser Rangefinder for Maritime Applications

Alasdair McInnes

DSTO-TR-0921

20000503 106

Characterisation, Analysis and Design Optimisation of a Wide Field-of-View Laser Rangefinder for Maritime Applications

Alasdair McInnes

Electronic Warfare Division
Electronics and Surveillance Research Laboratory

DSTO-TR-0921

ABSTRACT

This report describes analysis, performance modelling, validation and design optimisation that was carried out on a wide-angle rangefinder developed for non contact ship-ship distance measurement during Replenishment At Sea (RAS) operations. The results are applicable to the design and/or assessment of future wide angle rangefinders for this or other applications requiring direction-insensitive, accurate distance measurement. An iteration of design optimisation was carried out to determine the possible performance and likely physical dimensions of a system optimised for the RAS role, and also to provide a starting point for any future engineering development.

APPROVED FOR PUBLIC RELEASE

DEPARTMENT OF DEFENCE
DEFENCE SCIENCE & TECHNOLOGY ORGANISATION **DSTO**

DTIC QUALITY INSPECTED 3

Conditions of Release and Disposal

Characterisation, Analysis and Design Optimisation of a Wide Field-of-View Laser Rangefinder for Maritime Applications

EXECUTIVE SUMMARY

Replenishment at Sea (RAS) operations are manpower-intensive and relatively hazardous, causing the diversion of effort from manning important weapon or surveillance systems and increasing the risk to crew members involved. It is necessary to be able to monitor the distance between ships over short ranges (up to 50 m), in real time and with sufficient accuracy to detect small changes in relative heading. Two ships steaming on a parallel course are drawn together if the distance between them becomes too short, so to avoid collision the ship-to-ship range must be monitored closely. Currently this is achieved by sending a marked line from one ship to the other, requiring time, effort and exposure of personnel on deck.

DSTO was tasked by the Director of Naval Warfare (DNW) to develop a system that would provide a non-contact method of measuring ship-to-ship range during RAS operations, in order to relieve pressure on manpower and improve operational safety.

Such a system was developed and taken to trial, and was found to exceed performance expectations. This report describes subsequent detailed analysis, performance modelling, validation and design optimisation that was carried out in order to determine the performance possible from such systems. The modelling and analysis is applicable to any laser rangefinder system, and will be a useful tool for design of future systems and assessment of existing or proposed systems.

The analysis is particularly suited to scenarios in which the return is largely directed back at the source. This finds applicability in ranging from co-operative targets, and from optical sensors, which is relevant to countering surveillance or targeting sensors, including electro-optic missile seekers.

The optimised system design resulting from the analysis is extremely compact and considerably more capable than that taken to trial. It could be used as a baseline for engineering development, and such systems could be manufactured in Australia at minimal cost. No such system is fielded with any Defence Force to the author's knowledge. There is considerable pressure to reduce manning levels on decks of major surface combatants. This technology has the potential to play a part in future ship systems, as well as various other roles. Accordingly it is recommended that this technology be pursued by letting a contract for the design and fielding of several units for an extended period of evaluation.

Author

Alasdair McInnes
Electronic Warfare Division

Alasdair McInnes received his B.Sc.(Hons) from Glasgow University and his M.Sc. from St. Andrews University, Scotland, in 1982 and 1983 respectively. From 1983 to 1990 he worked at Barr & Stroud Ltd, (now Pilkington Optronics), Glasgow, Scotland. During that time he worked on laser induced damage of optical materials, sensor protection, and laser development. In 1990 he joined the Australian Defence Science and Technology Organisation, where he has worked on eyesafe lasers, diode pumping of solid state lasers, and laser systems.

Contents

1. Introduction

DSTO was tasked by DNW to develop a system that would provide a non-contact method of measuring ship-to-ship range during Replenishment at Sea (RAS) operations, in order to relieve pressure on manpower and improve operational safety. In September 1998 that system was taken to trial, aboard HMAS Perth and HMAS Melbourne, and was found to exceed performance expectations [1]. That system became known as the Electro-Optic Replenishment at Sea (EORAS) system. This report describes subsequent detailed analysis, performance modelling, validation and design optimisation that was carried out on the rangefinder system in order to determine the performance possible from such systems. The modelling and analysis is applicable to any laser rangefinder system, and will be a useful tool for design of future systems and assessment of existing or proposed systems.

The analysis is particularly suited to scenarios in which the return is largely directed back at the source, such as from a corner reflector or from an optical system. This finds applicability in ranging from co-operative targets, and from optical sensors being directed at the rangefinder, which is relevant to countering surveillance or targeting sensors, including electro-optic missile seekers.

2. Aims

The aim of developing a wide-angle rangefinder was to enable hands-free, accurate distance measurement between two moving platforms, without the need for pointing or tracking of the sensor. The aim of the analysis was to develop validated models of the performance of such systems, so that their suitability for future sensing applications may be assessed. Design optimisation was carried out to determine the possible performance and likely physical dimensions of a system optimised for the Electro-Optic Replenishment at Sea (EORAS) role, and also to provide a starting point for any future engineering development of the system [1]. The aims were met.

3. Replenishment Operations

Replenishment at Sea (RAS) operations are manpower-intensive and relatively hazardous, causing the diversion of effort from manning important weapon or surveillance systems and increasing the risk to crew members involved.

During RAS operations, two ships are required to steam on a parallel course at a distance of less then 50 m for a period of many minutes, while fuel, stores or personnel are transferred from one to the other. It is necessary to be able to monitor the distance

between the ships in real time and with sufficient accuracy to detect small changes in relative heading. Two ships steaming on a parallel course are drawn together if the distance between them becomes too short, so to avoid collision the ship-to-ship range must be monitored closely. Currently this is achieved by sending a marked line from one ship to the other, but this requires time, effort and exposure of personnel on deck. If a non-contact, real time method of range and range rate measurement could be implemented, crew safety and manpower effectiveness would be considerably enhanced.

4. System Description

The distance measurement function is based on a diode laser rangefinder. The laser diode emits a short pulse of light into a wide cone angle, which is reflected from a corner-cube reflector mounted on the other ship. The reflector may or may not be part of another such system. A receiver detects the return and the time between emission and detection is measured.

Use of a wide beam removes the need to point the laser accurately at a particular point on the other ship or track the ship's motion, but necessitates the use of corner reflectors to provide a strong return from a known location. The range measured is then the direct distance between the two units. As well as transmitting a wide beam, it is also necessary for the receiver to have a wide field of view so that all returns are detected.

5. Transmitter

The transmitter used is a multiple-emitter laser diode array. The output energy per pulse was measured to be 2.3 µJ and the FWHM pulse width was 33 ns. This equates to a peak power per pulse of 70 W. Figure 1 shows a trace of the temporal profile of the emitted pulse.
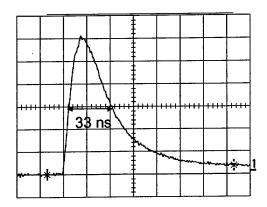
Figure 1: Temporal profile of laser pulse

To carry out each ranging operation, the laser emits a train of 1024 pulses at 11 kHz, the returns of which are processed to reduce the effect of background noise by approximately a factor of 30.

The natural divergence of the beam is specified by the manufacturer to be $30° \times 10°$, and this is increased to $30° \times 30°$ by splitting off portions of the beam and directing them at an angle to one another, as shown in Figure 2. Thus the final overall beam divergence is approximately $30°$ in horizontal and vertical planes, although the distribution is strongly peaked. Figure 3 and Figure 4 show spatial profiles of the raw diode output and the output after the beamsplitters, as transmitted by the system. It can be seen that the three lobes of the beam do not contain the same energy, indicating that the beamsplitter reflectivities could be further optimised. An additional effect of the beamsplitter unit is to increase the effective source size, making the system less vulnerable to occlusion of the transmitted beam by a single foreign body, such as dirt or salt encrusting.
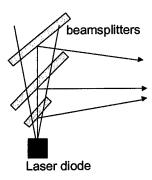
Figure 2: Beamsplitter arrangement
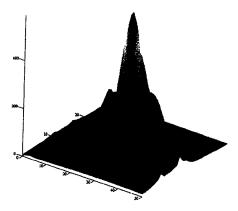
Figure 3: Raw laser diode spatial profile (horizontal axes scales in degrees)
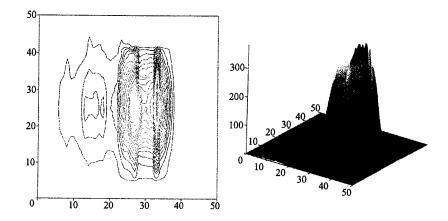
Figure 4: Spatial profile after beamsplitters, as transmitted (horizontal axes scales in degrees)

6. Reflectors

Corner cube reflectors are used to define the ranging point on the target, and to enhance the return signal. Corner cubes have the property of sending the intercepted part of the beam straight back to the source irrespective of the angle of arrival of the beam on the corner cube, without changing the divergence. The result is that the reflected beam is centred on the source aperture, with a diameter of twice that of the corner cube. This means that the receiver aperture must be positioned within this diameter in order to detect a return. Figure 5 shows the positioning of laser and receiver aperture in the EORAS unit, from which it can be seen that only a relatively

small percentage of the return finds its way into the receiver. This provides an opportunity for considerable enhancement in later versions.
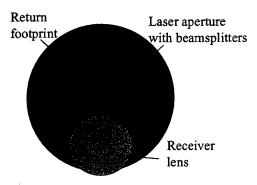
Figure 5 : Position of return footprint

Since the size of the return footprint from a corner cube scales with its size, there is no advantage in using larger corner cubes. Instead it is possible to increase the returned signal by using more corner cubes of the same size. The units trialled at sea had provision for up to four corner cubes, of which three were used on both units.

7. Receiver

7.1 Optical

In the receiver, a lens concentrates incoming radiation onto an array of 6 PIN photodetectors. An RG 850 filter is used to reject daylight, and the optical path is folded by a mirror to separate the detector and its electronics from the laser and its driver. This reduces transient electrical noise when the laser is fired (so-called "T-zero" noise). The arrangement of the aperture of the mirror, the lens and photodiodes is such that a 23 x 32 degree field of view (at half response) is obtained, in the vertical and horizontal direction respectively. Figure 6 shows the layout and Figure 7 the response as a function of angle.

The detectors are not positioned at the focus of the lens, as this would lead to a smaller field of view and possibly damage, if the sun entered the field. Instead an intermediate position is used which gives an optical concentration factor of around 2.8. It also mitigates any effect of gaps between the sensitive areas of the detectors. The total sensitive area of the detectors is around 42 mm².
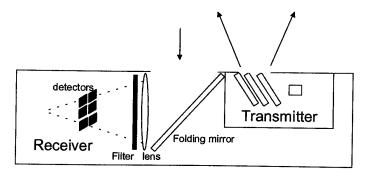
Figure 6: Layout of optical components
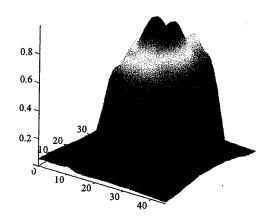
Figure 7: Response as a function of angle (degrees)

7.2 Electronic

Figure 8 shows a schematic of the receiver circuitry. The detectors are arranged in parallel, and biased at 29V. Being large in sensitive area, (in order to provide the necessary field of view), they are also large in capacitance. The in-circuit detector capacitance was measured to be around 220 pF, which agrees with the manufacturer's data sheet. When the sun is in the field of view, the bias drops to around 12 V, and the capacitance increases to around 350 pF. In practice it is observed that under these conditions the sensitivity of the receiver is reduced by approximately a factor of 3.

The large detector capacitance results in a receiver front-end that is not optimised for the laser pulse width used, as it cannot follow a 33 ns pulse. The peak signal is reduced by roughly half compared to the performance expected of a circuit with more appropriate capacitance. Therefore performance gains can be attained in this area by optimising the design of future versions.

The detector output is capacitively coupled into a transimpedance amplifier with a gain of 10000 volts/amp. This is followed by a variable gain stage, in which the gain is set to match the strength of the return by stepping it down to an appropriate level over the first 32 returns (which are not used in range extraction). A further amplification of 10 is applied before the signal is digitised for processing. The signal levels have been traced through the analogue part of the circuitry, and have been correlated with the expected levels in controlled optical experiments. Good agreement was found, and the models are detailed in Section 10.
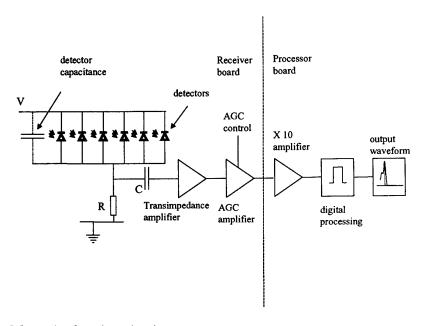
Figure 8: Schematic of receiver circuitry.

8. Hardware Deficiencies

The angular profile of the transmitted beam is highly non-uniform. This results in non-uniform range performance, and considerable scope for improvement.

As stated in Section 6, the receiver geometry is far from optimised for the application. The return beam falls in a circle centred on the laser diode aperture, of diameter 76 mm. The receiver aperture intercepts only a small fraction of this, and this is the primary deficiency of the current design.

The use of a lens and detector array combination imposes limits on the field of view through the laws of geometrical optics. Additionally the electrical configuration results in signal loss through mismatch of the receiver bandwidth and the laser pulse width.

A suggested approach to improving transmitted beam profile, transient electrical noise, enhancing receiver geometry, field of view and electrical performance is proposed and analysed in Sections 12 and 13.

9. Processing

9.1 Digitisation

Each return is digitised by an 8-bit A-D converter. The clock rate is 40 MHz, and 4-fold interleaving is used to increase this to an effective rate of 160 MHz, resulting in approximately 1m range resolution for the digitised waveform.

9.2 Averaging

Each return, after digitisation, results in a vector containing values representing the signal output during each time-slice of 6.25 ns. In each range measurement cycle, 1024 laser pulses are emitted at a rate of 11 kHz, and the returns summed vectorially. This leads to an enhancement in signal to noise ratio of approximately a factor of 30. This process is illustrated schematically in Figure 9.

After averaging, the output of the system is a vector containing the averaged returns. This must then be processed to extract a value for the range of the target.
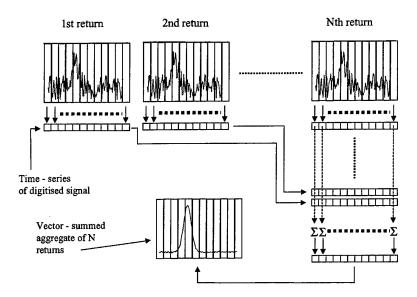
Figure 9: Vector summation of returns

9.3 Range Calculation

There are many techniques for extracting range data from a return waveform. In this case, the most important quality is repeatability of range reading under a variety of background conditions and signal strength, as might be encountered when ranging between moving ships. Background level could vary significantly on a timescale of several seconds if the sun were periodically in the field due to roll, and signal level could similarly change due to relative orientation. Absolute accuracy is not deemed so important, as the main parameter of interest is change in the range (range rate), rather than the actual value of separation between the ships.

9.3.1 Algorithm Development

In order to develop an optimised algorithm for range extraction under such conditions, laboratory measurements were conducted that allowed the simulation of a wide range of signal and background levels.

Figure 10 shows the arrangement used. The laser output was coupled into a fibre-optic cable, which provided a delay equivalent to a round trip of approximately 86 m (simulating a range of 43 m). This was sufficient to separate the return signal from any "T-zero" noise transients induced by the firing of the laser. It was necessary to prevent all leakage of laser light from around the fibre, as in a laboratory environment it is easily reflected into the receiver aperture, confusing the measurements.
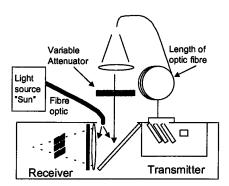
Figure 10: Algorithm development arrangement

The laser output from the fibre was directed into one half of the receiver aperture, through a set of filters that were used to vary the effective signal strength.

The other half of the receiver aperture was used to couple in a high-brightness fibre-optic light source, to simulate solar background. The level of background illumination was set by measuring the reduction in bias voltage on the photodetectors caused by pointing the receiver directly at the sun. This voltage drop was then induced in the laboratory by setting the brightness of the light source.

Measurements were carried out with the "sun" either on or off, at 4 values of AGC control voltage, and over a range of signal strength appropriate to the other settings.

80 output waveforms were generated and then used to evaluate a number of algorithms in terms of their range repeatability performance.

9.3.2 Algorithms Tested

The simplest form of range extraction algorithm is a threshold operation, where the time at which a preset threshold signal value is exceeded is deemed to be the elapsed time, and used to calculate the range. Such a technique can be made more a little more robust by averaging the times of the positive and negative-going crossings. However the technique is not suitable for this application due to the large range of signal strength, and also signal to noise ratio, encountered. A more robust algorithm is required that is insensitive to these variations.

Five different algorithms were tested against the range of waveforms generated in the laboratory. In each case the output is an x-value of some feature in the waveform, which is then converted to time after pulse emission, and hence range. The algorithms were;

- Centroid – the centroid of the entire waveform is calculated

- Gated centroid – the centroid of the waveform, starting after a "gate" of a certain number of points, is calculated. This discriminates against "T-zero" noise
- Correlation peak – the position of the peak of a correlation function (vector) of a second function is calculated. The other function in this case was 20 points around the peak of a "clean" waveform, ie. one in which the SNR was high and there were no saturation or other detrimental effects.
- Correlation centroid – as above but the centroid is calculated rather than the peak position.
- Gated correlation centroid – as in the correlation centroid but ignoring the first few (typically 25) points.

To select the most appropriate algorithm, the mean and the standard deviation of the range values produced by the different algorithms over the range of waveforms was calculated. It was found that the performance was markedly different depending on whether the "sun" was on or off, so these are examined separately. The results are shown in Table 1.

Table 1. Results of algorithm tests

	Centroid	Gated centroid	Correlation peak	Correlation centroid	Gated correlation centroid	"SUN"
Mean range (m)	55.6	42.5	41.6	44.8	43.7	OFF
Std. Dev. of range	4.7	1.8	0.5	8.2	1.1	OFF
Mean range (m)	49.6	52.5	43.9	51.2	56.1	ON
Std. Dev. of range	5.2	5.1	1.0	5.1	7.9	ON
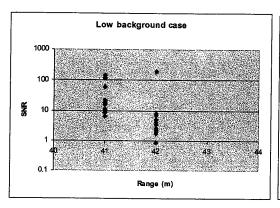
It can be seen that the lowest standard deviation in both high and low background conditions, which corresponds to the best repeatability, is provided by the correlation peak technique. Accordingly this was the one selected for implementation.

It should be noted that the mean value differs by 2.3 m between high and low background conditions, which could be a problem in some operational orientations. To compensate for this, the gated correlation centroid range result can be used as a test for high background, as it is typically different by 12 m between the two states, and an appropriate adjustment made to the range output. This was also implemented.

9.3.3 Algorithm Performance

The performance of the correlation peak algorithm was assessed in terms of its ability to extract the correct range in the presence of noise, using the waveforms previously generated as an input data set.

Figure 11 shows the range value returned as a function of SNR, for cases of high and low background illumination. These are treated separately as the offset has not been removed, and would tend to confuse the results.
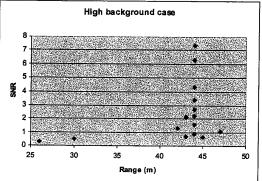
Figure 11: Range results vs. SNR

It can be seen that the range can be reliably extracted, to an accuracy of <1 time increment (1 metre in range) at SNR values down to 1 in low background conditions, and 2 in high background. This is deemed to be good performance, as in standard rangefinder modelling [2], the required SNR is typically taken to be more than 6. Therefore use of this algorithm increases the maximum range capability by a factor of 1.8 – 2.5 over that conventionally expected.

Figure 12 shows the raw waveform data and the correlation output for a variety of conditions. It can be seen that the correlation peak algorithm is effective at extracting returns from waveforms with very low SNR, but also can deal with strong signal returns. It should be noted that the width of the return pictured in Figure 12 (middle trace, left) corresponds to around 20 m in range, yet the algorithm returns the range value with a standard deviation of no more than 1 m, across all SNR values.

Result 45 m,
high background,
weak signal

Result 46 m,
high background,
strong signal

Result 45 m,
low background,
weak signal
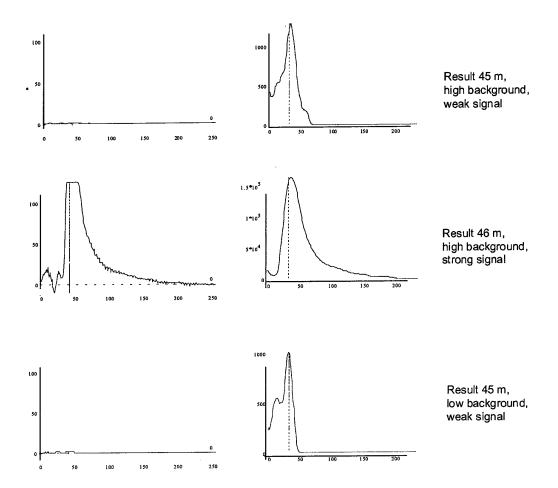
Figure 12: Raw data and correlation waveforms

10. Modelling

The range performance of the system has been modelled in detail. The aim of such modelling is to arrive at a validated model that can be used for design optimisation, and input to other laser rangefinder problems.

The process involves two distinct parts, signal modelling and noise modelling. The signal amplitude is modelled by following the signal contribution from generation through detection to output voltage. Noise is modelled by use of a commercial software package to predict the expected noise voltages. The minimum SNR that gives

valid range, as determined in Section 9 above, is then used to back-calculate the maximum expected range.

10.1 Signal

In the optical domain the signal is modelled in terms of power. The laser diode emits a pulse of energy E, and FWHM τ. This is approximated by a top-hat pulse, of constant power P, where

$$P = E/\tau.$$

This pulse is then emitted with an angular profile as shown in Figure 4. Knowledge of this distribution, the total peak power emitted and the angular resolution of the profile, allows calibration of the profile in W.sr^{-1}. The calibrated angular power density is denoted $H(\theta,\varphi)$. This is then propagated to a corner cube reflector at range R, which intercepts a fraction of the angular power density emitted in its direction determined by the solid angle it presents to the source. The power, P_{cc}, entering the corner cube of diameter D_{cc}, is

$$P_{cc} = H(\theta,\varphi) \cdot \pi (D_{cc} / 2R)^2$$

This amount of power is reflected, with reflectivity R_{cc}, into an area twice the size of the corner cube, centred on the source. If there is more than one corner cube, the reflected power scales with their number, N_{cc}. Thus the power density at the receiver is

$$H_{rec} = P_{cc} \cdot R_{cc} \cdot N_{cc} / (\pi D_{cc}^2)$$

The power reaching the detectors, P_{det}, is then determined by the effective sensitive area, which is influenced by the optical gain factor of the collection lens, the overlap of receiver aperture with return beam, and efficiency factors of the mirror, optics and filters. All these factors are lumped together and denoted A_{eff}, evaluated by measurement to be 118 mm^2.

The only other factors to be taken into account are the transmittance of the perspex window used on both transmitter and receiver (T_{window}), and the total reflectance of the beamsplitters (R_{bs}).

This allows us to write the power reaching the detectors as

$$P_{det} = H(\theta,\varphi) \cdot R_{cc} \cdot A_{eff} \cdot R_{bs} \cdot N_{cc} \cdot (T_{window} / 2R)^2$$

Power incident on the detectors is converted to current according to the responsivity, D, and the peak value is modified by the temporal response of the detector circuit, if

the bandwidth is less than that required to pass the pulse without attenuation. The effect of the temporal response can be described by defining an electrical efficiency η_e, which is the ratio of the peak current to that expected in the case of no attenuation. The detector capacitance is such in this case that the bandwidth is considerably less than optimum for the pulse width, resulting in a calculated value for η_e of 0.4.

The current pulse is input to a transimpedance amplifier of gain G, whose output is a voltage pulse of amplitude V given by

$$V = P_{det} \cdot \eta_e \cdot G$$

The signal is not traced further through the system as the noise is referenced to this point in the circuit.

10.2 Noise

The noise performance of the system is analysed by using the commercially available electronic design and analysis software P-SPICE™ [3]. Initially it was expected that the dominant noise term would be background-induced, due to the large field of view of the receiver. In practice it is found that the largest contribution is from the transimpedance amplifier.

Background induced noise is due to shot noise in the resistor through which photocurrent produced by dc illumination flows to ground. The value of this photocurrent can be high, in this system up to 0.5 mA. This results in a shot noise current of 30 nA in the 5 MHz bandwidth, which equates to a RMS background induced noise voltage of 0.3 mV at the output of the transimpedance amplifier.

Amplifier noise is due primarily to Johnson noise in the feedback resistor, and FET-induced noise. A simple analysis of the circuit did not give good agreement with the observed performance, so a P-SPICE model was constructed, which included the diodes as a current source, (both pulsed and DC), the transimpedance amplifier, including P-SPICE library modules for the active components, and also the subsequent AGC circuit. The result was that the noise not due to background was of the order of 1 mV RMS at the output of the transimpedance amplifier, and therefore the contribution due to DC illumination was of the order of 16 %.

Dominance of the amplifier noise is borne out by analysis of selected bench measurements (described in Section 9.3.1). Figure 12 (top and bottom traces) shows that the difference in noise with the "sun" on and off is almost negligible.

The effect of digital processing carried out after the analogue receiver circuitry was taken to be equivalent to reducing the noise by the square root of the number of samples.

10.3 System Performance Prediction

In Section 9.3.3 it was found that the selected algorithm was capable of extracting valid range data when the SNR value is as low as 1 in the low-background case and 2 with high background. Now that we can calculate the expected signal and noise in a given geometry, we can calculate the expected range performance, by evaluating the predicted maximum range as that resulting in a SNR of 1.

Figure 13 shows the maximum predicted range performance as a function of azimuth and elevation in the low-background case, using 3 corner cube reflectors. It can be seen that the predicted performance exceeds that experimentally measurable for a range of angles, as the system memory imposes a range limit of 213 m.
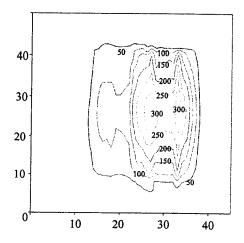
Figure 13: Maximum range contours for existing system (Note: this plot is shown rotated by 90 degrees – the field of view is greater in the horizontal plane).

11. Comparison of Results with Model

In order to validate the model, a further phase of laboratory measurements was carried out. In a carefully characterised setup, the signal was measured at the transimpedance amplifier output. Noise measurements were extracted from the earlier results described in Section 10.1. Finally predictions of overall system performance were compared with those observed both at sea and in DSTO tests.

11.1 Signal

The energy emitted per pulse was measured using a sensitive energy meter, a Laser Probe RjP-667, and found to be 2.3 µJ. Using the measured of pulse width value of 33 ns, this corresponds to a peak power of 70 watts. The angular distribution of the transmitted beam was measured using a computer controlled 2-axis rotation stage, in order to quantify $H(\theta,\varphi)$. A corner cube of diameter 38 mm, and estimated reflectivity of 0.9, was positioned at a range of 7 m from the unit, and the orientation of the rangefinder adjusted for peak signal. The transmittance of the perspex window was measured to be 0.92.

Under these circumstances the peak voltage at the output of the transimpedance amplifier was measured to be 350 mV. The model described in Section 10.1 predicts a signal of 354 mV, in excellent agreement. Experimental uncertainty is estimated to be of the order of 20% for the calculated signal voltage, and < 10% for the voltage measurement.

11.2 Noise

Noise values were measured on the digitally averaged output from the unit, by evaluating the standard deviation of the last 50 points in the waveform. It was then necessary to calculate the noise voltage at the output of the transimpedance amplifier that would give rise to such values, as it was found impractical to measure directly the noise at this point. This calculation assumes that the digital processing reduces the noise by the square root of the number of waveforms averaged. The resulting value is then modified to allow for two amplifier stages, one with a gain of 10 on the digital board, and the AGC amplifier. The combined effect of this is that one "unit" in the digital output is equivalent to approximately 1 mV of noise at the output of the transimpedance amplifier. Uncertainty of this value is estimated to be up to 30%.

In the measurements, it was found that the total noise at the output was approximately equal to one unit, so the noise at the point of comparison with signal is found to be approximately 1 mV. This is in good agreement with the result of the P-SPICE modelling described in Section 10.2.

11.3 System Performance

This is carried out for two sets of experimental data, measured field of view in the trial and maximum range with a single corner cube in outdoor tests at DSTO.

11.3.1 Field of View

In the trial, the maximum field of view was found by noting the times at which range data became invalid due to one ship being ahead or astern of the other, and viewing

the video record to measure the angular change between those events. In the trial report [1] the maximum field of view is evaluated to be 50° at a range of 40 m.

We can calculate the expected maximum field of view by examining Figure 13. We take the low-background case as the sun was not near the field of view of the receiver at the time of the measurement in the trial. The predicted field of view at 40 m is evaluated by finding the angular extent in the horizontal plane of the 40 m maximum range contour (not shown), which is approximately 38°.

This value is less than that measured, indicating that the model is conservative in its calculation of maximum range. This could be for a number of reasons. Propagation of estimated uncertainties of various quantities throughout the calculations results in a total uncertainty of SNR calculation of up to 40%, and even though comparisons with measured parameters generally find closer agreement, the resulting uncertainty in maximum range is approximately 15%. The minimum SNR for valid ranging may be considerably less than 1, as we have no data that shows an invalid range result due to low SNR in the low-background case (Figure 11). In separate tests it was found that the overall effect of high background on signal response of the system was to reduce the sensitivity by a factor of 3. Given that there is no significant increase in system noise due to high background (Figure 12), it might be reasonable to assume a minimum SNR in the low-background case of 1/3 of that obtained in high background, ie 0.67. However this would only lead to a modest increase in predicted field of view. Inaccuracy in the measurement of the field of view at sea by examining videotape of the remote ship is likely to be a significant contributor to any error.

11.3.2 Range

Comparing the predicted maximum range of the system with that observed is somewhat complicated by the highly non-uniform angular response, and the fact that the maximum predicted range performance exceeds the memory capacity of the system. It was achieved by reducing the non-uniformity of the response by transmitting only the beam reflected from the first beamsplitter. This also reduces the transmitted energy, and use of a single corner cube ensured that the predicted range at the peak of the angular response was well within the system's memory limit.

Under these circumstances we find that the predicted maximum range in low-background conditions is 130 m. The test range was limited to 120 m, so it was necessary to attenuate the return signal in order to simulate longer ranges. It was found that with no attenuation the system reliably gave valid ranges at 120 m. Use of the attenuator effectively increased the measurement range to 170 m, and valid ranges were returned in approximately 50% of cases. Reliable ranging was obtained at an effective range of 140 m, indicating that the model gives good agreement with system performance, and errs on the conservative side.

12. Design Optimisation

A number of deficiencies in the current design were described in Section 8. Now that a full understanding of the operation of the system has been developed, and the primary contributing factors determined and analysed, suggestions for improvement of the design can be made.

In order to optimise the design, we need a specification that is required to be met, and parameters that are required to be minimised or maximised, subject to boundary conditions.

The specification is taken from the original requirement from RAN, and observations of RAS evolutions while at sea. The system would need to provide range readings with a comfortable margin of signal, at ranges up to 50 m, and over a field of view of 50° x 30° (horizontal x vertical), in low and high background conditions. A comfortable margin of signal is defined as having range capability to 75 m in high background conditions.

Parameters to be maximised are, in decreasing order of importance:

- Horizontal field of view (≥ 50°)
- Vertical field of view (≥ 30°)

Parameters to be minimised are, in order of importance:

- Overall size of unit
- Cost / complexity

There are four main areas where significant improvement can be made; use of available face area, transmitted beam profile, receiver efficiency and detector electronic configuration.

In order to minimise overall size of the unit, maximum use of the available face area must be made. It should be primarily composed of source, receiver and reflectors.

12.1 Transmitter

The transmitted beam profile could be improved by propagation through a short length of beam homogeniser, which is comprised of a length of optical fibre of specific design. A range of homogenisers is commercially available with a variety of output profiles and shapes. The end of the homogeniser then acts as a secondary source whose divergence can be tailored by use of a suitable lens. This allows us to specify the output beam to be approximately rectangular, approximately uniform in profile and of any divergence we choose. A transmission loss may be allowed to account for coupling efficiencies throughout the arrangement.

Use of this technique allows greater physical separation and electrical isolation between transmitter and receiver, which should reduce the effect of "T-zero" noise.

12.2 Receiver

The receiver geometry could be significantly better matched to the return beam footprint, and efficiency of collection greatly improved. There are now commercially available detectors that combine a small detector with a lensed mount (similar to a high-brightness LED) and daylight filter that open up the possibility of using an array of detectors rather than an optical system. The array could be matched in area to the return beam footprint, centred on the transmit aperture. The effective collection area of each detector is approximately 10 mm², yet the actual sensitive area is only 1mm², giving substantial optical amplification while providing low capacitance. Individual detectors have approximately a 20° field of view (full-angle at half response), so the required system field of view may be obtained by mounting the detectors on an appropriately curved surface.

12.3 Detector Circuitry

In the existing design, receiver circuit performance is limited by the large capacitance of the detector, which leads to a front-end electrical efficiency of only 0.4, due to a mismatch of the electrical bandwidth to the laser pulse width. This could be increased by approximately a factor of two by optimising the detector capacitance. Use of an array of small detectors as described above would allow selection of the front-end bandwidth, by choosing the number of small detectors to be connected in parallel, and separately buffering a number of such clusters.

12.4 Optimisation

When considering optimisation of the system, it quickly becomes apparent that the parameters with greatest combined influence are the effective receiver area, and the number and size of corner cubes used.

A larger corner cube allows more of the outgoing radiation to be directed back to the receiver over a larger area, potentially allowing greater sensitive area. Use of multiple corner cubes scales the return signal linearly without affecting the return footprint. Given the symmetry of such a corner cube-based system, effective use of the available face area is achieved only with 4 or more corner cubes.

Use of multiple reflectors allows us to consider small corner cubes. The limit on this is the number and orientation of detectors within the return beam footprint. The absolute minimum would be when the return footprint overlaps the transmit aperture and enough space for a single ring of detectors outside. The detectors have a diameter of 5 mm, and the transmit aperture is unlikely to be smaller than 10 mm, so the footprint

would have to be 20 mm wide. This leads to a minimum corner cube size of 10 mm. However a single ring of detectors cannot provide the required horizontal field of view, since each has a field of view of 20°. To achieve a 50° field of view, a minimum of 3 detectors across the width of the footprint is needed. Given the symmetry of the system, a more practical minimum would be 4 detectors, which would give a flatter response profile and improved sensitivity. Such a geometry leads to a minimum corner cube diameter of 15 mm.

13. Performance Prediction for Optimised System

Having used physical constraints to define the basic optical design of the system, we can now model it in more detail to analyse the effect of changes to various parameters. The broad agreement between modelling and measurement described in Section 11 provides the necessary basis to extend the model to predict the performance of new geometries.

The arrangement chosen is one that maximises the proportion of face area occupied by active components. It has a central transmit aperture of 10 mm diameter, surrounded by an array of detectors, each of which is 5 mm in diameter, has a field of view of 20°, an effective collection area of 10 mm², and a capacitance of 2 pF. The array extends to the limit of the return beam footprint, as defined by the size of the corner cubes used. The detectors are individually angled to define the chosen field of view. For simplicity of modelling, the detector centres are defined to be on a square array. Packing density could be improved in practice, but a square array will give indicative values.

Input parameters to the model are the required fields of view in the horizontal and vertical planes and the size of corner cube reflectors. Outputs include the maximum range as a function of angle, which can be simplified to the horizontal and vertical widths of a chosen range contour.

The signal response is modelled by establishing the number, position and angles of the detectors for given fields of view and corner cube size, then evaluating the effective detector area for returns coming from a range of angles. Combining this with the transmitted beam profile, we can calculate the expected return signal over the angular range.

Noise is also affected by changes in the design. The background-induced noise is calculated by noting that the background scales with both the field of view and collection area. The noise associated with a single detector is calculated on this basis, then scaled by the root of the number of detectors. It is further increased by the increased front-end bandwidth, by a maximum of the root of the increase in electrical efficiency. One point to note is that as the field of view is increased, it becomes

increasingly likely that the sun will be within it. Amplifier noise is assumed to increase by $\sqrt{2}$ due to the increased bandwidth.

13.1 Results

The model was run for a number of sets of input parameters. Initially the design field of view was set at 50° x 30° (horizontal x vertical).

In order to determine the effect of transmitted beam profile, a number of different profiles were used –

- a "soft-edged" rectangular profile, which is as near as practicable to the ideal case,
- an elliptical Gaussian of 1/e widths equal to the desired FOVs, and
- an elliptical super-Gaussian of order 4 and the same 1/e width, which gives a flatter peak and sharper cut-off.

The latter might be the closest approximation to the profile obtainable with real components.

It was found that there is little overall difference between the above profiles. A summary for the super-Gaussian case of the fields of view (along the axes, for a range of 75 m in high background) and overall maximum range and number of detectors as a function of corner cube diameter is given in Table 2.

The primary consideration in this optimisation is to maximise the field of view, subject to the boundary conditions. In order to explore the limits of predicted performance, the model was run with increasing design fields of view, and the point at which the predicted performance was unable to provide that required taken as the limit. As might be expected, the Gaussian profile gives the least well-defined FOV boundary due to the gentler slope of the output profile. Those with a sharp cut-off in the output profile give a sharp cut-off in range performance. For this reason the Super-Gaussian design gave the widest fields of view for given optical geometries.

Table 2. Results for revised design with Super-Gaussian transmit profile.

Vert. FOV	Horiz FOV	Max. range (m)	No. of detectors	Dia. of CC (mm)
26	44	178	44	15
30	50	304	116	25
32	52	444	168	35

It is clear that the initial specifications are almost met by the smallest device with the

least number of detectors, thus minimising cost and complexity. Since the specifications are some 50% more exacting than the original requirement, and the model is known to underestimate performance, this design is thought to be the best suited of those explored.

An illustration of the proposed design is shown in Figure 14. The version shown has 15 mm corner cube reflectors, 40 detectors mounted on a convex surface and a 10 mm transmit aperture. It could be expected to have a maximum range capability of > 170 m combined with a field of view of at least 44 x 26 degrees (H x V). The face area of this unit is only some 50 mm square, and the drawing is close to actual size.
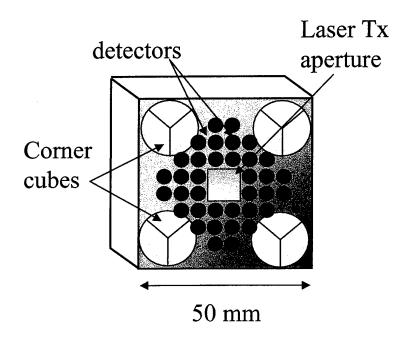
Figure 14: Improved design

The maximum predicted range performance as a function of angle is shown in Figure 15. Comparing this with Figure 13 we see that the proposed design gives a more uniform response, a wider field of view, and a maximum range more appropriate to the task. (Note that Figure 13 is shown rotated by 90 degrees). If greater performance is required, the design can be scaled up with larger corner cubes and more detectors.
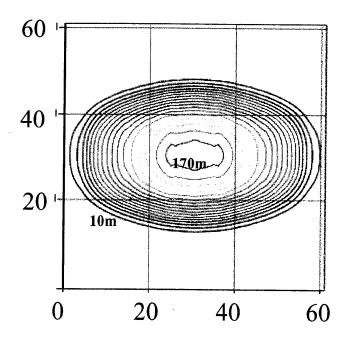
Figure 15: Maximum range vs angle (°) for design shown. Contours are in 10 m intervals

14. Conclusions

The diode-laser based rangefinder used in the EORAS trial has been analysed in detail. A model of its performance has been developed and validated. An iteration of design optimisation has been carried out, which shows that rangefinders of this class can provide a compact, eyesafe, hands-free solution to short-range distance measurement problems in a high background, mobile environment. While developed for a maritime application, land and airborne uses can be envisaged.

15. Recommendations

It is anticipated that such systems could be manufactured in Australia at minimal cost. No such system is fielded with any Defence Force to the author's knowledge. There is pressure to reduce manning levels on decks of major fleet units, and studies have been conducted showing a trend towards zero men on deck [4]. This technology is applicable now and has the potential to play a part in future surface ship systems, as well as various other roles. The (unoptimised) system has been trialed at sea with positive results.

It is recommended that this technology be pursued by letting a contract for the design and fielding of several units for an extended period of evaluation.

16. Acknowledgments

The prototype unit was designed and fabricated by Laser Integrated Technologies, Hallett Cove, SA. Members of the DSTO trial and development team included Alan Davidson and Douglas Carr of EWD, and Bruno Russo of LOD. Assistance with P-SPICE modelling from Terence Yeow and Rod Watson is gratefully acknowledged.

17. References

1. "Trial ESRL 12/97 – The EORAS Trial" A McInnes, DSTO-CR-0102, 1998

2. IR/EO Systems Handbook, vol 6. C S Fox (ed). SPIE press.

3. P-SPICE™, ORCAD Inc., Beaverton, OR, USA.

4. Jane's International Defense Review, Sep 98, p43ff

Characterisation, Analysis and Design Optimisation of a Wide Field-of-View Laser
Rangefinder for Maritime Applications

Alasdair McInnes

(DSTO-TR-0921)

AUSTRALIA

Number of Copies

1. DEFENCE ORGANISATION

Task sponsor: Director of Naval Warfare, Level 2, Bldg 89/90,
Garden Island Dockyard, Woolloomooloo, NSW   1

S&T Program

Chief Defence Scientist	⎫	
FAS Science Policy	⎬ shared copy	1
AS Science Corporate Management	⎭	

Director General Science Policy Development   1

Counsellor Defence Science, London   Doc Data Sheet

Counsellor Defence Science, Washington   Doc Data Sheet

Scientific Adviser Policy and Command   1

Navy Scientific Adviser   1

Scientific Adviser - Army   Doc Data Sheet
1 x distribution list

Air Force Scientific Adviser   1

Director Trials   1

Aeronautical and Maritime Research Laboratory

Director   1

CMOD   1

CMPD   1

K Gaylor, MPD   1

Electronics and Surveillance Research Laboratory

Director   Doc Data Sheet
1 x distribution list

Chief, Electronic Warfare Division   1

Research Leader, EO Electronic Warfare   1

Research Leader, System Integration & Operation   1

Head, EO Systems & Technologies   1

27

Alasdair McInnes	1
J Richards	1
S Rees	1
A Davidson	1
B Russo, LOD	1

DSTO Library

Library Fishermens Bend	1
Library Maribyrnong	1
Library Salisbury	2
Australian Archives	1
Library, MOD, Pyrmont	Doc Data sheet

Capability System Staff

Director General Maritime Development	Doc Data Sheet
Director General C3I Development	Doc Data Sheet

Navy

SO (Science), Director of Naval Warfare, Maritime Headquarters Annex, Garden Island, NSW 2000	Doc Data Sheet

Army

ABCA Office, G-1-34, Russell Offices, Canberra	4
SO (Science), DJFHQ(L), MILPO Enoggera, Queensland 4051	Doc Data Sheet
NAPOC QWG Engineer NBCD c/- DENGRS-A, HQ Engineer Centre Liverpool Military Area, NSW 2174	Doc Data Sheet

Intelligence Program

DGSTA, Defence Intelligence Organisation	1
Manager, Information Centre, DIO	1

Corporate Support Program (libraries)

OIC TRS, Defence Regional Library, Canberra	1
US Defense Technical Information Center,	2
UK Defence Research Information Centre,	2
Canada Defence Scientific Information Service,	1
NZ Defence Information Centre,	1
National Library of Australia	1

UNIVERSITIES AND COLLEGES

Australian Defence Force Academy, Library	1

Head of Aerospace and Mechanical Engineering,
Serials Section (M list), Deakin University Library, Geelong, 3217   1

Senior Librarian, Hargrave Library, Monash University   1

Librarian, Flinders University   1

OTHER ORGANISATIONS

NASA (Canberra)   1

AGPS   1

State Library of South Australia   1

Parliamentary Library, South Australia   1

<p align="center">OUTSIDE AUSTRALIA</p>

ABSTRACTING AND INFORMATION ORGANISATIONS

INSPEC: Acquisitions Section Institution of Electrical Engineers   1

Library, Chemical Abstracts Reference Service   1

Engineering Societies Library, US   1

Materials Information, Cambridge Scientific Abstracts, US   1

Documents Librarian, The Center for Research Libraries, US   1

INFORMATION EXCHANGE AGREEMENT PARTNERS

Acquisitions Unit, Science Reference and Information Service, UK   1

Library -
Exchange Desk, National Institute of Standards and Technology, US   1

SPARES   6
Total number of copies: 60

Page classification: UNCLASSIFIED

DEFENCE SCIENCE AND TECHNOLOGY ORGANISATION DOCUMENT CONTROL DATA	1. PRIVACY MARKING/CAVEAT (OF DOCUMENT)

2. TITLE Characterisation, Analysis and Design Optimisation of a Wide Field-of-View Laser Rangefinder for Maritime Applications	3. SECURITY CLASSIFICATION (FOR UNCLASSIFIED REPORTS THAT ARE LIMITED RELEASE USE (L) NEXT TO DOCUMENT CLASSIFICATION) Document (U) Title (U) Abstract (U)

4. AUTHOR(S) Alasdair McInnes	5. CORPORATE AUTHOR Electronics and Surveillance Research Laboratory PO Box 1500 Salisbury SA 5108

6a. DSTO NUMBER DSTO-TR-0921	6b. AR NUMBER AR-011-182	6c. TYPE OF REPORT Technical Report	7. DOCUMENT DATE January 2000

8. FILE NUMBER U 9505-17-164	9. TASK NUMBER NAV 94/385	10. TASK SPONSOR DNW	11. NO. OF PAGES 42	12. NO. OF REFERENCES 4

13. URL ON WORLD WIDE WEB http://www.dsto.defence.gov.au/corporate/reports/DSTO-TR-0921.pdf	14. RELEASE AUTHORITY Chief, Electronic Warfare Division

15. SECONDARY RELEASE STATEMENT OF THIS DOCUMENT

APPROVED FOR PUBLIC RELEASE.

OVERSEAS ENQUIRIES OUTSIDE STATED LIMITATIONS SHOULD BE REFERRED TO DOCUMENT EXCHANGE, PO BOX 1500, SALISBURY, SA 5108, AUSTRALIA

16. DELIBERATE ANNOUNCEMENT

No limitations

17. CASUAL ANNOUNCEMENT	Yes

18. DEFTEST DESCRIPTORS
Laser range finders
Range finding
Modelling
Replenishment at sea
Ship to ship

19. ABSTRACT
This report describes analysis, performance modelling, validation and design optimisation that was carried out on a wide-angle rangefinder developed for non contact ship-ship distance measurement during Replenishment At Sea (RAS) operations. The results are applicable to the design and/or assessment of future wide angle rangefinders for this or other applications requiring direction-insensitive, accurate distance measurement. An iteration of design optimisation was carried out to determine the possible performance and likely physical dimensions of a system optimised for the RAS role, and also to provide a starting point for any future engineering development.

Page classification: UNCLASSIFIED